ACS APPLIED BIO MATERIALS



Article

# Modulation of macrophages differentiation by nanoscale-engineered geometric and chemical features

Akash Bachhuka, Rahul Madathiparambil Visalakshan, Cheryl Suwen Law, Abel Santos, Heike Ebendorff-Heidepriem, Srikanth Karnati, and Krasimir Vasilev

*ACS Appl. Bio Mater.*, **Just Accepted Manuscript** • DOI: 10.1021/acsabm.9b01125 • Publication Date (Web): 16 Feb 2020



## Just Accepted



is published by the American Chemical Society. 1155 Sixteenth Street N.W., Washington, DC 20036

# Modulation of macrophages differentiation by nanoscale-engineered geometric and chemical features

*A. Bachhuka[1,2#*], R. Madathiparambil Visalakshan[3#], C.S. Law[1,2,4], A. Santos[1,2,4], H. Ebendorff-Heidepriem[1,2], S. Karnati[5], K. Vasilev[3, 6*]*

*1 ARC Center of Excellence for Nanoscale BioPhotonics (CNBP), The University of Adelaide, SA 5005, Adelaide, Australia*

*2 Institute for Photonics and Advanced Sensing (IPAS), The University of Adelaide, SA 5005, Adelaide, Australia.*

*3 Future Industries Institute, University of South Australia, Mawson lakes Campus, SA, 5095, Australia.*

*4 School of Chemical Engineering, University of Adelaide, Engineering North Building, SA 5005 Adelaide, Australia.*

*5 Institute for Anatomy and Cell Biology, Julius Maximilians University, Koellikerstrasse 6, Wuerzburg, 97070, Germany.*

*6 School of Engineering, University of South Australia, Mawson lakes Campus, SA, 5095, Australia.*

*# Authors with equal contribution*

**Corresponding author email address: akash.bachhuka@adelaide.edu.au*

**Corresponding author email address: Krasimir.vasilev@unisa.edu.au*

KEYWORDS: plasma polymerization, nanoporous substrates, surface chemistry, pro-inflammatory cytokines, anti-inflammatory cytokines, foreign body response, wound healing.

ABSTRACT

Macrophages differentiation into M1 (inflammatory) and M2 (healing) phenotypes plays a vital role in determining the fate of biomaterials. The biophysical properties of the extra-cellular matrix are known to affect macrophage behavior. Mimicking these special biophysical properties of the extra-cellular matrix have led to increasing interest in biomaterial constructs with tailor-engineered surface nanotopographical

and chemical properties. However, significant gap of knowledge exists in the role played by the combinational effect of surface nanotopography and chemistry. To address this gap, we have fabricated nanoporous surfaces of controlled pore size (30, 65 and 200 nm) and lateral spacing with uniform outermost surface chemistry tailored with amines ($NH_2$), carboxyl (COOH-) and hydrocarbon ($CH_3$-) functionalities. We show that the combinatory effects of surface properties can direct the differentiation of macrophages to the pro-healing M2 phenotype. This is most evident on the surface containing featuring nanopores of 200 nm and -COOH functionality. Overall, the concentration of pro-inflammatory cytokines significantly decreases while the concentration of anti-inflammatory cytokines increases many folds on nanotopographically, and chemically modified surfaces compared to their planar counterparts. Our data provides pioneering knowledge that could provide pathways to tuning inflammatory and foreign body responses and instruct the design of tailor-engineered biomaterial implants to enable better clinical outcomes.

## INTRODUCTION

The biggest performance challenge that biomaterial implants face is modulation of the host immune response. Immediately upon implantation, adsorption and desorption of different proteins occur on the biomaterial's surface, a phenomenon known as the Vromann effect[1-2]. This governs the subsequent biological phenomena underlying binding and activation of waves of innate immune effector cells such as neutrophils, macrophages, dendritic cells, mast cells, granulocytes and natural killer cells[3-8]. Of all these, macrophages are an important class of immune cells which attempt to eliminate the foreign body (i.e. biomaterial implant) by fusing among themselves to form foreign body giant cells (FBGC). Macrophages are a critical component of the host immune response, both to implants and microorganisms, through their phagocytic activities[9]. Macrophages are considered as 'plastic' cells, being categorized into 'M1' and 'M2' phenotypes based on their respective roles[8, 10-12]. M1-activated macrophages are key elements in inflammation and responsible for 'cleaning the site' by expressing pro-inflammatory cytokines such as tumor necrosis factor (TNFα) and interleukin (IL6 and

IL1β). Conversely, the M2-activated macrophages produce anti-inflammatory cytokines (Arginase, IL10 and IL1RA) and are involved in wound healing and remodeling.

Recent studies by our group and others have shown that macrophage adhesion, phagocytic activity and cytokine production can be modulated by using biomaterial surface properties such as chemistry and nanotopography. These engineering tools can be effectively used to modulate inflammatory responses by biomaterial surfaces with tailored properties[13-17]. This provides exciting opportunity for the rational design of biomedical constructs to modulate and elicit desired immunological responses. For example, our work utilizing 'hill-like' nanotopography of 16 nm, 38 nm and 68 nm demonstrated that the scale of nanofeature significantly affected immune cells attachment and expression of inflammatory markers[13-15]. The effect of nanotopography was further modulated by the outermost surface chemistry, revealing a complex picture of mutually dependent parameters but also an opportunity to harness surface properties to design and guide inflammatory responses to biomaterials. We have also recently reported that 'hill-like' nanotopography induced conformational changes to adsorbed fibrinogen leading to unfolding and presentation

of normally hidden peptide sequences that activate the MAC-1 receptor of inflammatory cells[17].

In this work, we further expand the knowledge in the field and reveal the combinational role of nanopores and surface chemistry on modulating immune cell responses. As model substrata, we employed anodic alumina (NAA) which provides a nanoporous surface with hexagonally distributed nanopores. The geometric features of these NAA substrates can be precisely controlled by altering the fabrication conditions. NAA-based implants are not envisaged for developing brain implants due to potential leaching of aluminium ions under physiological conditions. However, NAA is recognized as a biocompatible material and has been intensively used to develop orthopaedic and dental implants [18,19]. Many studies have reported on the use of NAA-coated implants (e.g. orthopaedic, dental, coronary, etc.) and immunoisolation, showing reduced leaching of aluminium ions under physiological conditions[20]. NAA surfaces have also been engineered as active drug-releasing coatings in orthopaedic, dental and coronary implants and in immunoisolation[20-21]. Pioneering osteogenesis studies demonstrated the biocompatibility of NAA, suggesting that its nanoporous structure provides key cues in bone cell adhesion and osseointegration[22-24]. *In vitro*

immunoisolation studies performed onto NAA surfaces suggest that this nanoporous material does not generate significant complement activation. However, *in vivo* transient inflammatory response was observed for unmodified and PEG-functionalized NAA surfaces upon implantation into the peritoneal cavity of rats[20]. Reduction in granulation along with the existence of blood vessels in the tissue surrounding the NAA implant indicated complex inflammatory consequences that require further elucidation. Furthermore, the interplay of nanotopography and surface chemistry in macrophage differentiation has not been comprehensively investigated. To unravel these phenomena, the outermost surface chemistry of NAA with varying porous structure was tailored by a thin layer of functional polymers deposited by plasma. A key benefit of plasma polymerization is that, it generates coatings of desired physicochemical properties in an arbitrary substrate, without requiring any pre-modification of the surface[25] compared to techniques such as LbL or SAMs[26]. The method consists of a single step, occurring within minutes and does not require solvents which provides benefit in terms of time costs[27-30]. Moreover, these coatings can also be deposited on complex structures including micro and nano particles[16, 31-34]. Immune responses were evaluated on these nanotopographically and chemically

modified surfaces by measuring the expression of pro- and anti-inflammatory cytokines from macrophages.

## MATERIALS AND METHODS

### Materials:

Aluminium foils (99.9997% purity and 0.32mm thick) were purchased from Goodfellow Cambridge Ltd. (UK). Oxalic acid ($H_2C_2O_4$), perchloric acid ($HClO_4$) and chromic acid ($H_2CrO_4$), were supplied by Sigma-Aldrich (Australia). Ethanol ($C_2H_5OH$, EtOH), sulfuric acid ($H_2SO_4$) and phosphoric acid ($H_3PO_4$) were purchased from ChemSupply (Australia). Ultrapure Milli-Q® water (18.2 mΩ·cm) was utilized to prepare all aqueous solutions.

Fabrication of Nanoporous Anodic Alumina:

Aluminum substrates were cleaned under sonication in a bath of EtOH and Milli-Q® water for 15 min each before anodization, and dried under air stream. The surface of cleaned Al substrates was electropolished in an electrolyte of $HClO_4$ and EtOH 1:4 (*v:v*) at 20 V and 5 $^oC$ for 3 min. This process was performed in an electrochemical reactor with a circular window of ~1 cm in diameter. Three types of nanoporous anodic alumina (NAA) substrates with tuned geometric features of nanopores were fabricated by two-step anodization[35-38]: i) NAA produced in sulfuric acid (NAA-Su, 30 nm), ii) NAA fabricated in oxalic acid (NAA-Ox, 65 nm), and iii) NAA anodized in phosphoric acid (NAA-Ph, 200 nm). The first anodization step was performed for 20 h in 0.3 M sulfuric

acid at 6 °C for NAA-Su, 0.3 M oxalic acid at 6 °C for NAA-Ox, and 0.1 M phosphoric acid for NAA-Ph at 1 °C, with anodization voltages of 25, 40 and 195 V, respectively. The resulting NAA films with disordered nanopores at the top were selectively removed by wet chemical etching in 0.2 M $H_2CrO_4$ and 0.4 M $H_3PO_4$ at 70 °C for 3 h. Then, we performed the second anodization step under the same conditions as during the first step but for 2 h. The final nanopore size in the NAA films was precisely tuned by by wet chemical etching in $H_3PO_4$ 5 *wt* % at 35 °C for 8, 18 and 30 min for 35 nm, 65 nm and 200 nm samples, respectively.

Plasma Polymerization:

A plasma reactor with a 13.56 MHz generator was utilized to modify NAA substrates with desired surface chemistry[27]. Nanoporous membranes were cleaned under oxgen plasma for 2 minutes at a power of 50W. Methyl oxazoline, acrylic acid and octadiene were utilized to overcoat the surface of NAA substrates with a 5nm thin layer of plasma polymer coating. Surface coatings of methyl oxazoline, acrylic acid and octadiene were deposited using a power of 40, 10 and 20 W, respectively, while the deposition time was kept constant at 20 s for all three monomers.

Scanning Electron Microscopy:

The geometrical features of the NAA substrates were established by field emission gun scanning electron microscopy (FEG-SEM FEI Quanta 450). Image J was utilized for processing FEG-SEM images.

X-ray photoelectron spectroscopy:

Elemental composition of the plasma surface coatings deposited onto the surface of the NAA substrates were determined using XPS. A Spec SAGE XPS spectrophotometer with a monochromatic Mg radiation source was operated at 10 kV and 20 mA to record all XPS spectra over 0-1000eV at a pass energy of 100eV and resolution of 0.5 eV. Survey spectra were then utilized to quantify atomic percentage of the elements present in the polymers. Neutral C1s carbon peak at binding energy (BE) of 285.0 eV was used as a reference to correct all other BE. All spectra were quantified using casaXPS.

Ellipsometer:

Silicon wafers were kept adjacent to the NAA substrates and plasma coated using the same parameters. A variable angle spectroscopic ellipsometer (J. A. Woollam Co.

Inc.) was used to measure the thickness of the polymer coatings. Reference silicon wafer was used for calibration and then all measurements were performed over a wavelength range of 250 to 1100 nm at 10nm increment at different angles from 65$^{o}$ to 75$^{o}$ at an interval of 5$^{o}$. The data obtained was quantified using Cauchy model. 3 measurements per sample were performed to obtain the average thickness, which were reported to have less than 10% experimental error.

Cell Culture:

THP-1 cells (Human monocytes) were grown in RPMI 1640 (Sigma Aldrich) with 1% (*v/v*) penicillin/streptomycin (Life Technologies) and 10 % fetal bovine serum (FBS, Thermo Scientific) and were then used for immune studies. An incubator set at 37 °C containing 5% $CO_2$ was used for maintaining cells and growth media was changed at 80% confluency (i.e. every 3 days).

Inflammatory response of macrophage:

Phorbol-12-myristate 13-acetate (PMA, 100ng/ml) was used to differentiate THP-1 cells into dTHP-1 (macrophages), according to the previously reported protocol[39-40]. Cells were treated for 48 h with media containing PMA and for another 24 h with fresh

media without PMA. Differentiated dTHP-1 macrophage cells were seeded on unmodified and modified NAA substrates at a density of 1 x $10^5$ cells $ml^{-1}$ and grown overnight for cell attachment. Once the cells were attached, the media was changed with fresh media containing 1μg $ml^{-1}$ LPS (lipopolysaccharide) to activate the macrophages. Cells were exposed with LPS for further 6 h and conditioned media were collected for quantification of cytokine production[41]. After collecting the media, macrophage cell counts were performed using trypsin and hemocytometer to quantify the number of cells that produced cytokines on each surface. Pro- and anti-inflammatory cytokines [IL-12p70, TNF-α, IL-6, IL-1β, IL-12p40, IL-23, IFN-γ, IP-10, IL-4, IL-10, Arginase, and TARC] were quantified using LEGENDplex human macrophage/microglia Panel (13-plex) and ELISA kits (BioLegend, San Diego, CA, USA) following the manufacturer's instructions.

Statistical Analysis:

Graph Pad prism 8 was used to quantify all statistical analysis using a 1-way ANOVA with Dunnett's multiple comparison test. The data obtained from all measurements (n=9) was presented as mean ± standard error mean (SEM).

RESULTS

Fabrication of NAA substrates having defined porous structure and outermost surface chemistry

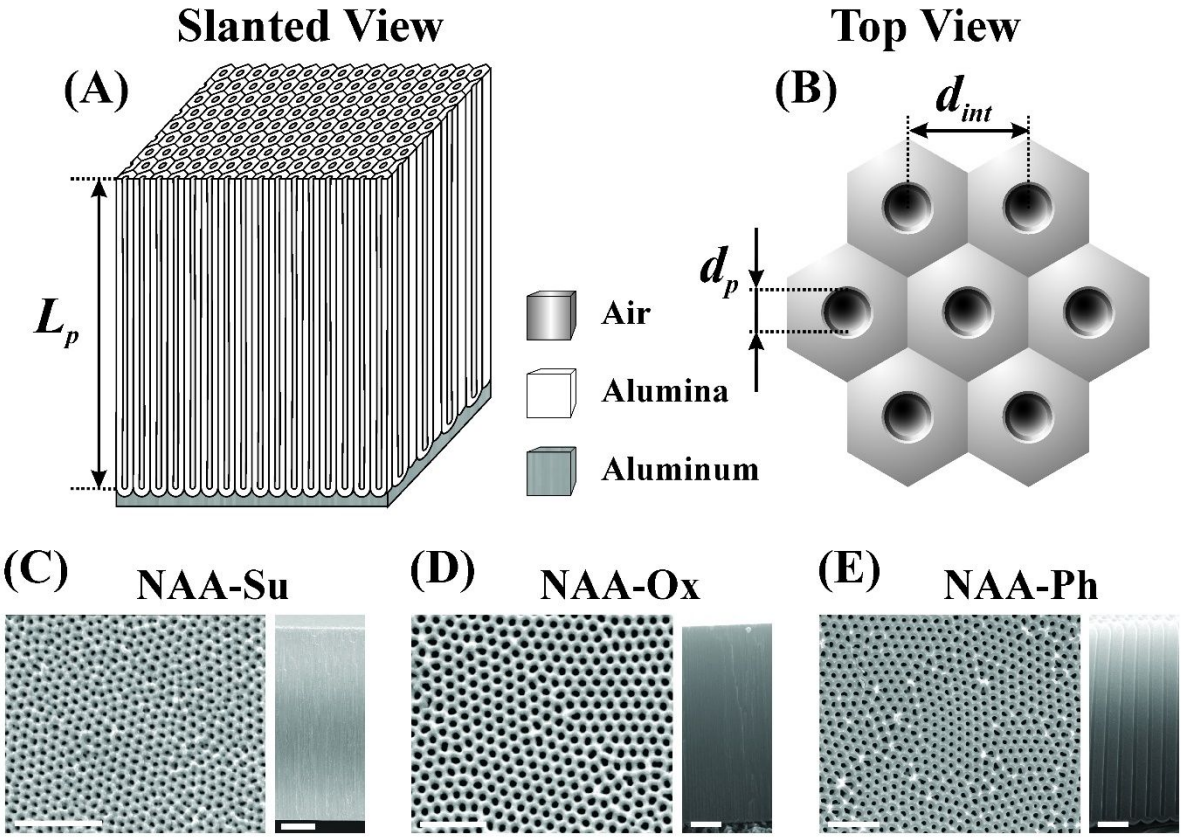


**Figure 1:** Geometric parameters of NAA substrates produced by two-step anodization. A,B) Slanted and top view schematics of a NAA substrate with details of geometric parameters (i.e. nanopore diameter $d_p$; nanopore length $L_p$; interpore distance $d_{int}$). C-E) Top (left) and cross-sectional (right) FEG-SEM images of NAA produced in sulfuric (scale bar (left) = 500 nm; scale bar (right) = 2 μm), oxalic acid (scale bar (left) = 500

nm; scale bar (right) = 1 μm), and phosphoric acid (scale bar (left) = 2.5 mm; scale bar (right) = 1 μm), respectively.The geometric parameters of NAA films (i.e. nanopore diameter $d_p$; nanopore length $L_p$; interpore distance $d_{int}$; and pore density $r_p$; **Figures 1A and B**) were measured through FEG-SEM image analysis. **Figures 1C–E** show representative FEG-SEM images of the cross-section and top surface of NAA films fabricated in this study[35-38]. **Figures 1C–E** show cross-sectional FEG-SEM images of NAA films with straight cylindrical nanopores grown perpendicularly to the underlying aluminum substrate. These nanopores feature a closed oxide barrier layer at their bottom (**Figure 1A**). In average, the nanopore length of NAA-Su, NAA-Ox and NAA-Ph substrates under the fabrication conditions used in our study were $L_p$ = 13.1 ± 0.5, 6.1 ± 0.4 and 7.5 ± 0.3 μm, respectively. The top surface of NAA substrates shows an array of nanopores of uniform size and distribution arranged in a self-organized hexagonal pattern (**Figures 1C–E**). The average nanopore diameter and interpore distance for NAA-Su, NAA-Ox and NAA-Ph substrates were $d_p$ = 30 ± 2, 65 ± 4 and 200 ± 4 nm and $d_{int}$ = 66 ± 3, 105 ± 5 and 449 ± 24 nm, respectively. The pore densities (i.e. number of nanopores per unit area) were $r_p = 2.65 \times 10^{11}$, $1.05 \times 10^{11}$ and $5.73 \times 10^9$ cm$^{-2}$ for NAA-Su, NAA-Ox and NAA-Ph substrates, respectively.

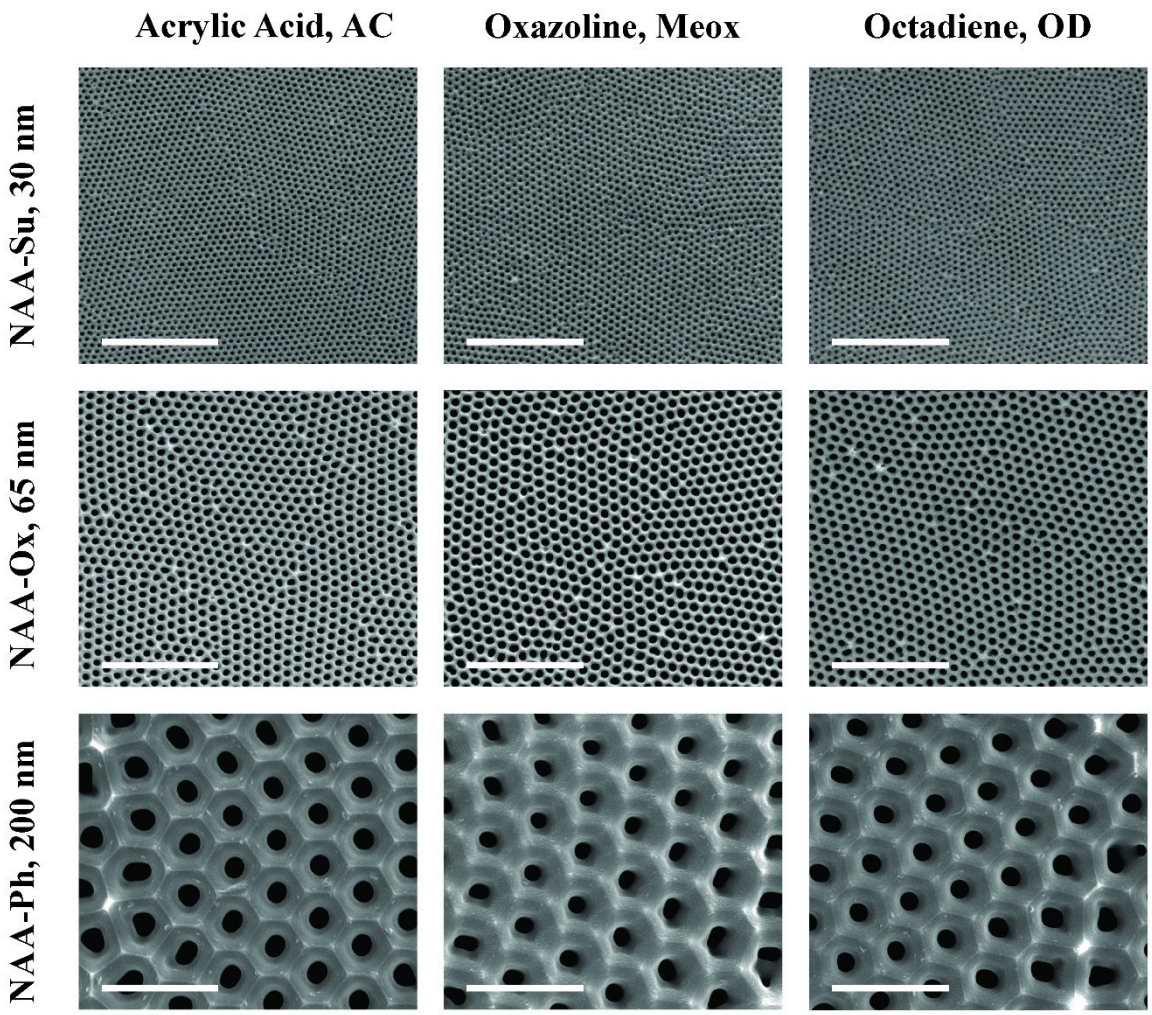


**Figure 2:** FEG-SEM image of nanoporous anodic alumina with three different pore sizes, 30 nm, 65 nm and 200 nm (scale bars = 1 μm) overcoated with three different chemistries (acrylic acid, methyl oxazoline and octadiene).

NAA substrates with desired outermost surface chemistry was obtained by overcoating 5 nm thick layer of plasma polymers obtained from different monomers

such as acrylic acid, methyl oxazoline and octadiene (ACpp, Meoxpp, ODpp).These surface coatings were chosen as they represent chemical compositions consistent with that of biological matter such as in amino acids, extra-cellular matrix and proteins (i.e. COOH- (ACpp), $NH_2$- (Meoxpp) and $CH_3$- (ODpp)[42-43]. All these coatings have negative surface charges in aqueous medium at physiological pH = 7.4 as Meoxpp and ODpp coatings are slightly negatively charged -18 mV and -19 mV, respectively, whereas the ACpp coatings had the highest negative charge of -28 mV (**Figure S1**)[44-45]. The different chemistries of the coatings result in different wetting characteristics, as indicated by water contact angles of 35° for ACpp, 60° for Meoxpp and 85° for ODpp (**Figure S2**)[17, 46]. The thickness of the plasma polymer films was tailored to be of 5 nm, in order to preserve as much as possible the original nanoporous structure. We know from our published work that plasma polymer films of 5 nm and above are continuous and pinhole-free, allowing us to preserve the nanotopography generated by the NAA substrates and thus study the combinational effect of nanotopography and surface chemistry[25, 47]. FEG-SEM images of overcoated NAA substrates are shown in **Figure 2**. The images demonstrate that the nanopores retain their original shape and

the surface morphology (i.e. nanopore diameter) is not affected by the outermost surface chemistry.

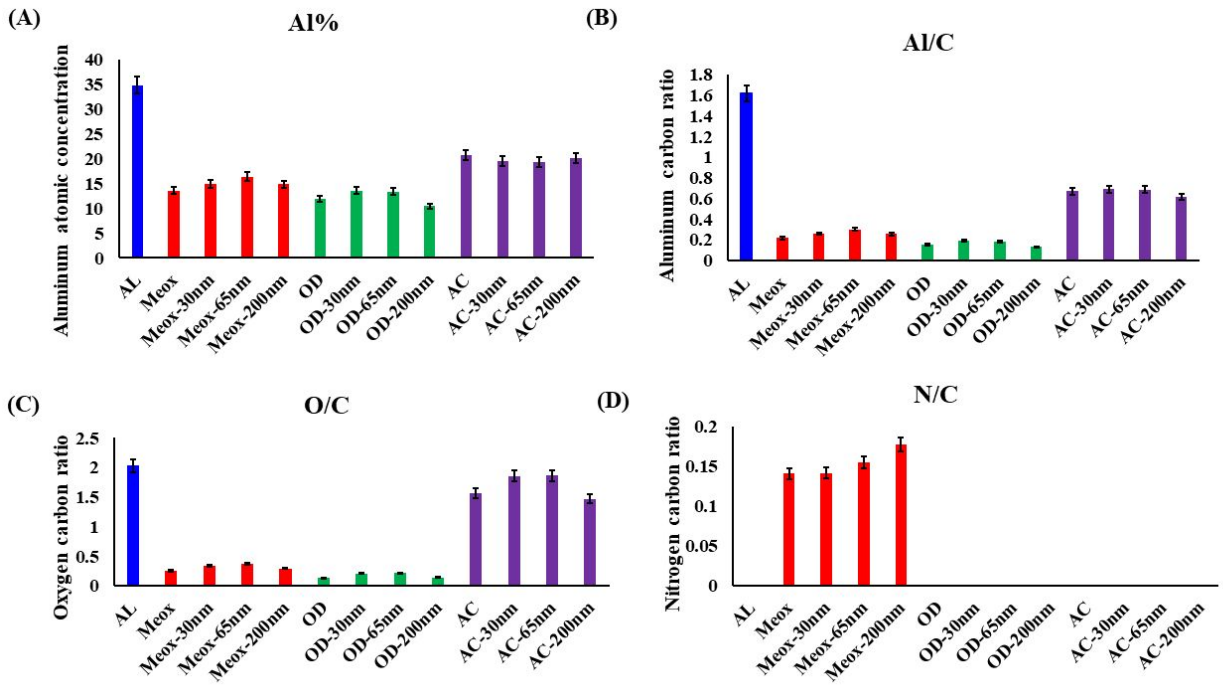


**Figure 3:** Surface chemical composition determined by XPS. Atomic percentage of element of interest on NAA substrates modified by plasma deposited surface coating from methyl oxazoline, octadiene and acrylic acid chemistries. (A) aluminum, (B) aluminum carbon ratio, (C) oxygen carbon ratio and (D) nitrogen carbon ratio.

The surface chemical composition of the coatings deposited by plasma polymerization on NAA substrates was characterized by XPS. The unmodified NAA substrates had 35 atomic percent of aluminum (**Figure 3A**). After deposition of a 5 nm thin plasma

polymer coating of Meoxpp, ODpp and ACpp, the atomic percentage of aluminum decreased by half, which indicates that the coatings were successfully deposited on the NAA substrates. Furthermore, the aluminum to carbon (Al/C) and oxygen to carbon (O/C) ratios decreased by one fourth in case of Meoxpp and ODpp coated nanoporous and NAA substrates as compared to their uncoated counterparts (**Figures 3B and C**). This is due to the high concentration of carbon present in the molecules of these monomers. Whilst Al/C ratio decreased by half and O/C ratio remained the same in ACpp overcoated NAA substrates compared to their uncoated analogs (**Figures 3B and C**). This is due to high concentration of oxygen present in the structure of acrylic acid. Moreover, alumina membrane has a top oxide layer which leads to high O/C ratio in case of uncoated alumina surface. The nitrogen by carbon (N/C) ratio is presented in **Figure 3D**. Nitrogen was detected only in case of Meoxpp and not in case of ODpp and ACpp coated surfaces constant with the chemical structure of the precursors.

Inflammatory responses (pro-inflammatory and anti-inflammatory) on different chemistry and nanoporosity

Macrophages play a central role in the host response to implanted biomaterials. These cells have the capability to polarize into M1 (inflammatory) and M2 (wound healing) phenotypes, which further generate an array of pro-inflammatory and anti-inflammatory cytokines, respectively. In this study, inflammatory responses to surface chemistry and nanoporosity (individually and in combination) was assessed in culture of macrophage dTHP-1 cells, obtained from differentiated THP-1 cell line. The results are presented in **Figures 4** and **5**.

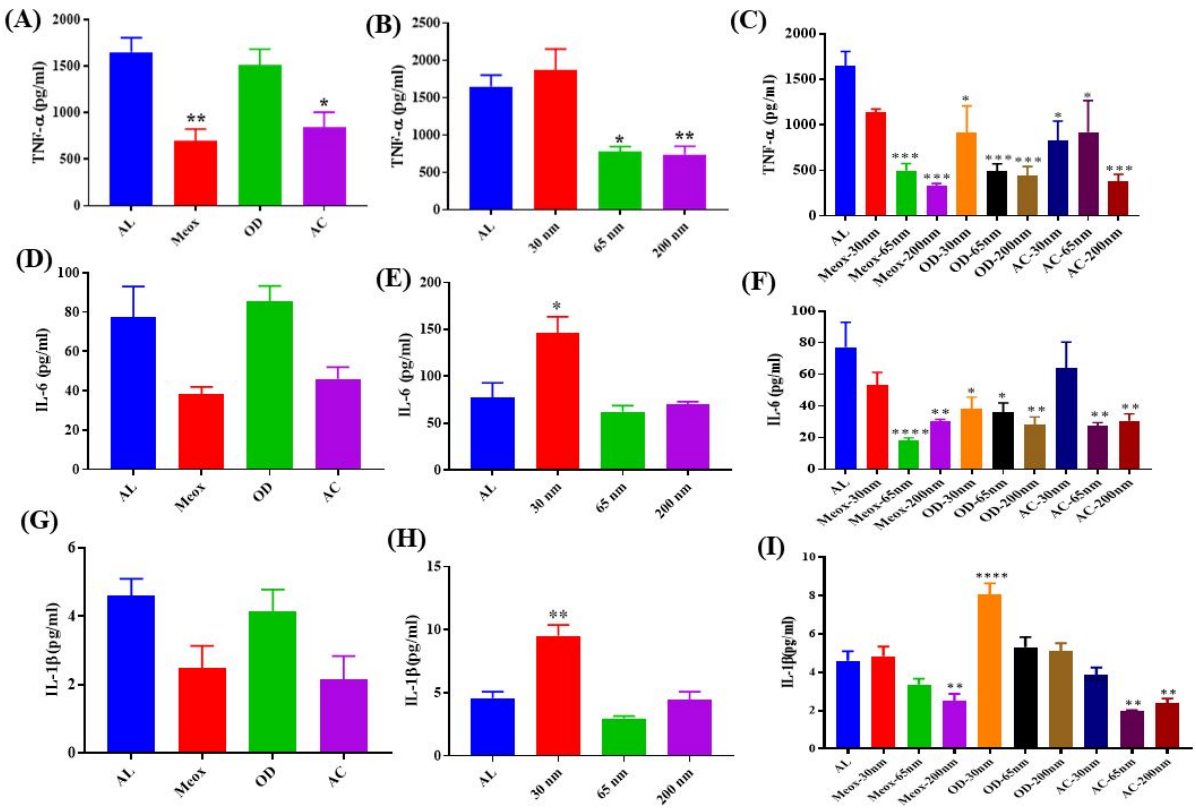

**Figure 4:** Expression of pro-inflammatory cytokines (TNFα, IL-6, and IL-1β) from macrophages stimulated by LPS (1μg/ml) to nanoporous alumina surfaces with different pore size and surface chemistry, as determined using Legendplex ELISAs. TNFα, IL-6, and IL-1β expression on nanoporous alumina modified with methyl oxazoline (Meox), octadiene (OD) and acrylic acid AC (A, D & G)), uncoated alumina with different pore sizes 30 nm, 65 nm and 200 nm (B, E &H), and from NAA modified with Meoxpp, ODpp and ACpp (C, F&I). * = $p<0.05$, ** = $p<0.01$ and *** = $p<0.001$

An overall reduction in cytokine expression levels was observed upon addition of a combination of nanoporosity and chemistry compared to the uncoated aluminium membranes (**Figure 4**). In the case of Meoxpp (** = $p<0.01$) and ACpp (* = $p<0.05$) coated surfaces, a significant reduction in the concentration of the cytokine tumor necrosis factor alpha (TNFα) was observed, while only a moderate reduction in concentration of interleukin-6 (IL-6) and interleukin-1β (IL-1β) was observed as compared to aluminum control surfaces (**Figures 4 A, D and G**). Upon addition of nanoporosity, a significant increase in the concentration of all three cytokines (TNFα, IL-6 and IL-1β) was observed on 30 nm surfaces, while the cytokine expression

decreased significantly on surfaces with larger pore size (i.e. 65 nm and 200 nm) (**Figures 4 B, E and H**).

The combination of nanoporosity and surface chemistry led to an overall significant decrease in the concentration of proinflammatory TNFα and IL-6 cytokines (compared to the control aluminum surfaces (**Figures 4 C, F and I**). Though an overall decrease in cytokines level was observed, the chemistries in combination with large pore size (200 nm) showed a more prominent decrease in the cytokine concentration compared to same chemistries on smaller pore sizes (i.e. 65 nm and 30 nm). Furthermore, nanoporous surfaces overcoated with Meoxpp and ACpp showed significant reduction in expression of all three pro-inflammatory cytokines compared to planar surfaces as well as to nanoporous surfaces with ODpp overcoating. The most significant reduction in the inflammatory cytokines was observed in case of Meoxpp and ACpp overcoated 200 nm (large pore diameter) surface. In case of nanoporous surfaces overcoated with ODpp chemistry, the expression of TNFα and IL-6 cytokines decreased significantly with the increase in pore size while an overall increase in the concentration of IL-1β was observed on these surfaces compared to planar alumina surfaces.

Table 1. Heat map summarizing the results obtained from ANOVA analysis performed to differentiate the individual effect of nanotopography and chemistry in the combination of the two, in case of pro-inflammatory cytokines expression.

| Biomarkers | Nanotopography | Chemistry | Combination |
|---|---|---|---|
| TNFα | 84% | 2% | 14% |
| IL-6 | 79% | 7% | 14% |
| IL1β | 32% | 66% | 2% |

Our experimental data shows (Figure 4) that the combination of nanotopography and chemistry has a synergistic effect on pro-inflammatory cytokine expression. However, to determine, the weighted impact of individual surface parameters in case of combination of t nanotopography and chemistry, a two way ANOVA was performed. The results presented in Table 1 were plotted by using the F0 values presented in supplementary Table S1. The ANOVA analysis demonstrates that in the case of TNFα and IL-6 nanotopography plays a much more significant role (83.9 % and 78.9%, respectively) compared to surface chemistry (1.9% and 6.7% respectively). Whereas, in case of IL-1β, both nanotopography (32.2%) and chemistry (66%) appear to be

important, however, surface chemistry has more prominent effect than nanotopography.

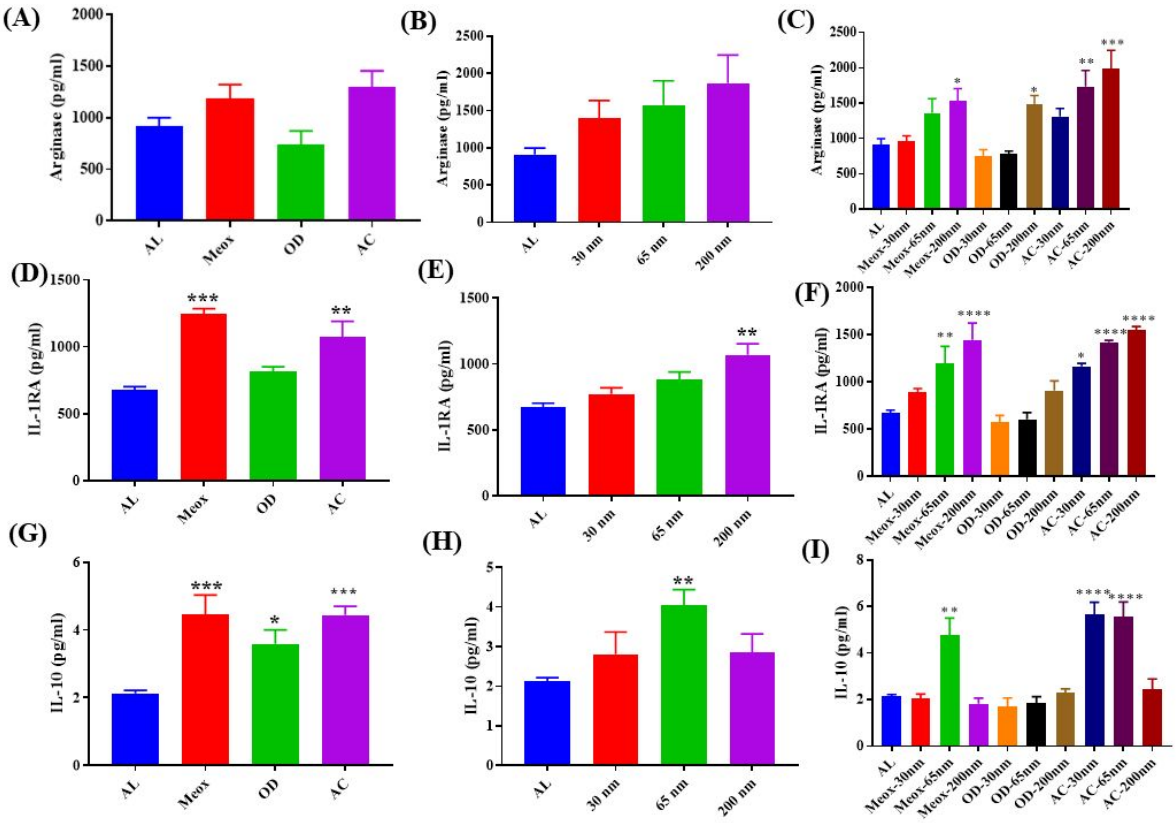


**Figure 5:** Expression of anti-inflammatory cytokines (Arginase, IL-1RA and IL-10) from macrophages stimulated by LPS (1µg/ml) to nanoporous alumina surfaces with different pore size and surface chemistry, as determined using Legendplex ELISAs. Cytokines Arginase, IL-1RA and IL-10 on nanoporous alumina modified with oxazoline (Meox), octadiene (OD) and acrylic acid (AC) plasma polymer (A, D &G)), alumina

with different pore sizes 30 nm, 65 nm and 200 nm (B, E &H), and from NAA modified with Meox, OD and AC (C, F&I). * = p<0.05, ** = p<0.01 and *** = p<0.001

An overall increment in anti-inflammatory cytokine concentration upon combination of nanoporosity and chemistry for all surface chemical modifications was observed (**Figure 5**). Meoxpp and ACpp coated surfaces displayed a significant increase in the concentrations of the cytokines, interleukin 1 receptor antagonist (IL-1RA) and interleukin-10 (IL-10), and only a moderate increment in concentration of arginase compared to aluminum control surfaces (**Figure 5 A, D and G**). Upon addition of nanoporosity, the concentration of IL-1RA increased significantly on surfaces with larger nanopores (200 nm) compared to counterpart surfaces with smaller nanopores (30 nm and 65 nm). While an increase in the concentration of IL-10 was more significant on 65 nm compared to 30 nm and 200 nm surfaces, and only a moderate increase in concentration of arginase (as compared to aluminum control surfaces) was observed (**Figures 5 B, E and H**).

The combination of different nanoporosity with these chemistries led to an overall significant increase in the concentration of the anti-inflammatory cytokines (arginase, IL1RA and IL-10) compared to the control aluminum surfaces (**Figures 5 C, F and I**).

Although, an overall increase in cytokines level was observed, the chemistries in combination with large pore size showed a more prominent increase in the cytokine concentration compared to chemistries on smaller pore size. Furthermore, anti-inflammatory cytokines increased to a much greater extent on nanoporous surfaces overcoated with Meoxpp and ACpp overcoated surfaces compared to ODpp overcoated nanoporous surfaces. The most significant increase in the expression of Arginase and IL1RA was observed in case of Meoxpp and ODpp overcoated 65 nm and 200 nm surfaces. While the most significant increase in the concentration IL-10 was observed in case of ACpp overcoated 30 nm and 65 nm surfaces.

Table 2. Heat map summarizing the obtained results from ANOVA analysis performed to differentiate the individual effect of nanotopography and chemistry in the combination of the two, in case of anti-inflammatory cytokines.

| Biomarkers | Nanotopography | Chemistry | Combination |
|---|---|---|---|
| Arginase | 48% | 49% | 3% |
| IL1RA | 27% | 72% | 1% |
| IL10 | 27% | 55% | 18% |

Two-way ANOVA analysis was performed to determine the weighted contribution of individual surface properties. The results in Table 2 were obtained by using the F0 values from supplementary Table S2. Table 2, clearly demonstrates that in the case of Arginase, IL1RA and IL10 both chemistry and nanotopography plays a significant role. However, in case of IL1RA, chemistry is three times more significant than nanotopography while in case of IL10, chemistry is only twice as significant as nanotopography.

## DISCUSSION

It is well established that different surface features play a critical role in modulating inflammatory responses [13-17]. However, the effect of these surface features on macrophages are still not well known. Macrophages become activated into 'M1' and 'M2' phenotype and expresses (pro and anti) inflammatory cytokines on its interaction with the biomaterial. While an initial pro inflammatory response to biomaterials generated by M1 macrophages is desired, its prolonged expression results in chronic inflammatory events followed by the formation of FBGC and failure of biomaterial implant. In addition, 'M2' phenotype expresses anti-inflammatory cytokines which

promotes tissue remodeling and aids in vascularization of regenerative biomaterials, inhibiting fibrous capsule formation. This suggests that controlling the fate of macrophage polarization is beneficial in retaining the integrity and normal functioning of the biomaterial implant. Therefore, understanding macrophage polarization through modulation of surface features has critical implications on the design and engineering of implantable biomaterials. This study reveals that a combination of surface nanoporosity with tailored surface chemistry can be readily used to modulate macrophage polarization by modulating the secretion of pro-inflammatory and anti-inflammatory cytokines.

NAA substrates were fabricated by two-step anodization to tune the geometric features of nanopores with precision[35-38]. A thin layer of Meoxpp, ODpp and ACpp (~5 nm) was deposited onto these nanoporous surfaces to generate desired uniform surface chemistries to further modulate macrophage responses. Using this approach, we were able to generate 15 independent types of surfaces with unique combinations of nanoporosity and chemistry. FEG-SEM and XPS analysis were used to establish the geometric and chemical features of the nanoporous substrates.

Our data demonstrates that the expression of pro-inflammatory cytokines decreased while anti-inflammatory cytokines increased on Meoxpp and ACpp coated surfaces, and the effect was boosted by combining these chemistries with increasing surface nanoporosity (30<65<200 nm). This is consistent with previous studies showing that hydrophilic -COOH surfaces can reduce inflammatory responses and fibrotic encapsulation[48-49]. Our previous studies also demonstrated that the combination of nanotopography (nanohills) with the -COOH surfaces reduced the level of expression of proinflammatory cytokines [14] and fibrotic capsule thickness[16] while increasing the expression of collagens[47]. Furthermore, the results presented in this paper indicate that the expression of cytokines can be modulated to a greater extent by using nanoporous surfaces with same chemistry compared to gold nanoparticles nanotopography surfaces with the same chemistry[14]. It is noteworthy that the cell numbers were same across all 15 substrates (**Figure S3 and S4**). Therefore, the decrease in pro-inflammatory signals or the increase in anti-inflammatory signals were not affected by adherent cells.

Furthermore, the levels of TNFα decreased significantly on Meoxpp and ACpp coated surfaces as well as on nanoporous surfaces with greater pore size compared to

uncoated alumina membranes. But the reduction in IL-6 and IL-1β expression was only observed upon combination of nanoporosity with surface chemistry. Additionally, IL-1RA and IL-10 increased significantly on Meoxpp and ACpp surfaces and remained unchanged on different nanoporous surfaces compared to uncoated alumina membranes. However, concentration of arginase only increased when a combination of nanoporosity with chemistry was utilized. Interestingly, hydrophobic ODpp surfaces showed no change in inflammatory responses (pro and anti). Also, expression of TNFα decreased while IL-1RA increased, but there was no change observed in the concentration of IL-6, IL-1β, Arginase and IL-10 on surfaces with greater nanoporosity (30<65<200 nm).

ODpp and nanoporous surfaces alone have been known to enhance inflammatory responses and fibrotic encapsulation around biomaterials[49-52]. On the contrary, our data indicates a significant reduction in the expression of TNFα and IL-6, and an increase in the expression of arginase when ODpp and large surface pores are used together. This suggests that surface nanoporosity or surface chemistry cannot be used alone as a tool to modulate immune responses. A possible explanation for nanoporosity mediated macrophage polarization could be nanotopography induced

orientation and conformational changes of adhered proteins[53-54], exposing unknown cell-surface receptors, causing unprecedented cellular behavior[17].

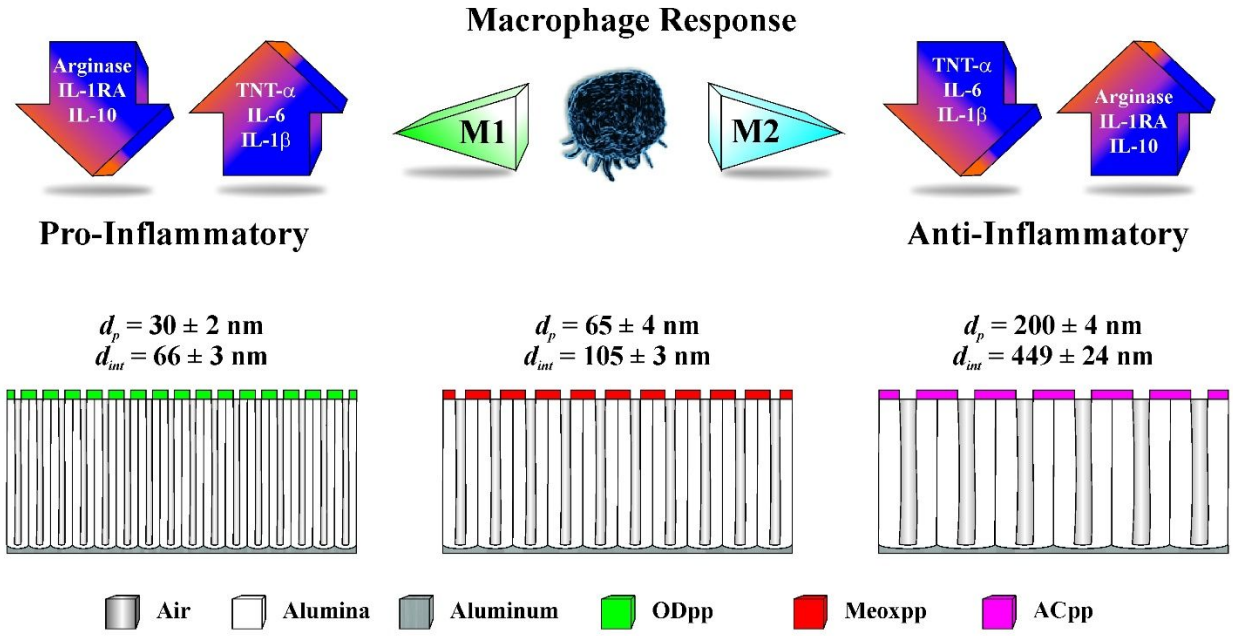


**Schematic 1.** Schematic representation of macrophage polarization (M1 and M2 phenotypes) on chemically and nanotopographically modified surfaces.

One of the biggest problems with medical devices is fibrosis or fibrous encapsulation[55-58]. Several strategies involving addition of growth factors[59-62], surface chemical modifications[46, 63-65] or the addition of surface nanotopography[13, 66-68] have been explored to address these problems. The data presented here suggest that the combinatorial effect of surface nanoporosity and surface chemistry can be used to control macrophage differentiation by modulating pro-inflammatory and anti-

inflammatory cytokines. For example, large pores and ACpp based outermost surface chemistry was shown to reduce expression of proinflammatory cytokines (**Figure 4**) and increase the production of arginase (**Figure 5**) suggesting differentiation to M2 type macrophages which contribute to improved healing. This has been further illustrated in **schematic 1**. To the best of our knowledge, this is the first comprehensive study, demonstrating that macrophage differentiation can be controlled by utilizing the right combination of surface nanoporosity and chemistry. As pro-inflammatory cytokines decreased, and anti-inflammatory cytokines increased on -COOH surfaces with large nanopores. Such surfaces can be utilized to fabricate biomaterials that can tune immune responses to enhance implantation site healing and can be used to establish a base for the future rational design of biomaterial implants.

## CONCLUSION

In this study, the role of surface nanoporosity and chemistry in controlling macrophages polarization into ‘M1’ and ‘M2’ phenotypes was assessed. Controlled surface nanotopography was generated by utilizing three different sizes of surface pores (30, 65 and 200 nm). Whereas, desired outermost surface chemistry on NAA

substrates was generated by coating 5 nm plasma polymer layer obtained from different monomers such as methyl oxazoline, 1, 7 octadiene and acrylic acid. This model system enabled the evaluation of the interplay between surface nanotopography and chemistry. We have shown that the concentration of pro-inflammatory cytokines (TNFα, IL-6 and IL-1β) decreased significantly on nanoporous surfaces featuring large nanopores and having Meoxpp and ACpp surface coatings compared to surfaces with smaller pore sizes and methyl group rich chemistry (OD). Furthermore, the concentration of anti-inflammatory cytokines (Arginase, IL-1RA and IL-10) increased significantly on large nanoporous surfaces with Meoxpp and ACpp coatings. Our data suggests that the macrophage differentiation can be controlled by selecting desired combinations of surface nanoporosity and chemistry. The knowledge obtained from this study provides cues that could aid in tuning foreign body responses and will eventually facilitate the rational design of biomaterial implants and constructs.

## ASSOCIATED CONTENT

### Supporting Information

The Supporting Information is available free of charge on the ACS Publications website at DOI:

Zeta Potential Measure (Figure S1) and water contact angle (Figure S2) of chemically modified surfaces. Macrophage cell count (Figure S3 and S4) on chemically and nanotopographically modified surfaces.

AUTHOR INFORMATION

*Corresponding Authors:

Dr Akash Bachhuka

ARC Center of Excellence for Nanoscale BioPhotonics, Institute for Photonics and Advanced Sensing, Faculty of Science, The University of Adelaide, South Australia, Australia, 5005.

Phone: (61) 424446844

Email: akash.bachhuka@adelaide.edu.au

Professor Krasimir Vasilev

Division of Information Technology, Engineering and the Environment, Future Industries Institute, University of South Australia, Mawson Lakes Campus, South Australia, Australia, 5095.

Phone: (61) 8 8302 5697, Fax: (61) 8 8302 5689

Email: krasimir.vasilev@unisa.edu.au

## AUTHOR CONTRIBUTIONS

The manuscript was written through contributions of all authors. All authors have given approval to the final version of the manuscript.

## ACKNOWLEDGMENT

KV thank to ARC grant ARC DP15104212, NHMRC for Fellowship APP1122825 and the Humboldt Foundation for the Humboldt Fellowship for Experienced Researchers.

AB, AS and HEH thank to ARC grant ARC CE140100003.

## REFERENCES

1. Vroman L, Adams A, Fischer G, Munoz P. Interaction of high molecular weight kininogen, factor XII, and fibrinogen in plasma at interfaces. Blood. 1980; 55 (1): 156-159.

2. Hirsh SL, McKenzie DR, Nosworthy NJ, Denman JA, Sezerman OU, Bilek MMM. The Vroman effect: Competitive protein exchange with dynamic multilayer protein aggregates. Colloids Surf. B. Biointerfaces. 2013; 103: 395-404.

3. Nimeri G, Öhman L, Elwing H, Wetterö J, Bengtsson T. The influence of plasma proteins and platelets on oxygen radical production and F-actin distribution in neutrophils adhering to polymer surfaces. Biomaterials. 2002; 23 (8): 1785-1795.

4. Nimeri G, Majeed M, Elwing H, Öhman L, Wetterö J, Bengtsson T. Oxygen radical production in neutrophils interacting with platelets and surface-immobilized plasma proteins: Role of tyrosine phosphorylation. J. Biomed. Mater. Res. A. 2003; 67A (2): 439-447.

5. Wetterö J, Bengtsson T, Tengvall P. Complement activation on immunoglobulin G-coated hydrophobic surfaces enhances the release of oxygen radicals from neutrophils through an actin-dependent mechanism. J. Biomed. Mater. Res. 2000; 51 (4): 742-751.

6. Lynn AD, Kyriakides TR, Bryant SJ. Characterization of the in vitro macrophage response and in vivo host response to poly(ethylene glycol)-based hydrogels. J. Biomed. Mater. Res. A. 2010; 93A (3): 941-953.

7. Zhao Q, Topham N, Anderson JM, Hiltner A, Lodoen G, Payet CR. Foreign-body giant cells and polyurethane biostability: In vivo correlation of cell adhesion and surface cracking. J. Biomed. Mater. Res. 1991; 25 (2): 177-183.

8. Christo SN, Diener KR, Bachhuka A, Vasilev K, Hayball JD. Innate Immunity and Biomaterials at the Nexus: Friends or Foes. BioMed Research International. 2015; 2015:1155-78.

9. Martinez FO, Sica A, Mantovani A, Locati M. Macrophage activation and polarization. Front. Biosci. 2008; 13 (1): 453-61.

10. Mosser DM. The many faces of macrophage activation. J. Leukoc. Biol. 2003; 73 (2): 209-212.

11. Mantovani A, Sica A, Sozzani S, Allavena P, Vecchi A, Locati M. The chemokine system in diverse forms of macrophage activation and polarization. Trends Immunol. 2004; 25 (12): 677-686.

12. Martinez FO, Helming L, Gordon S. Alternative Activation of Macrophages: An Immunologic Functional Perspective. Annu. Rev. Immunol. 2009; 27 (1): 451-483.

13. Chen Z, Bachhuka A, Han S, Wei F, Lu S, Visalakshan RM, Vasilev K, Xiao Y. Tuning chemistry and topography of nanoengineered surfaces to manipulate immune response for bone regeneration applications. ACS Nano. 2017; 11 (5): 4494-4506.

14. Christo SN, Bachhuka A, Diener KR, Mierczynska A, Hayball JD, Vasilev K. The role of surface nanotopography and chemistry on primary neutrophil and macrophage cellular responses. Advanced healthcare materials. 2016; 5 (8): 956-965.

15. Christo S, Bachhuka A, Diener KR, Vasilev K, Hayball JD. The contribution of inflammasome components on macrophage response to surface nanotopography and chemistry. Sci. Rep. 2016; 18 (6): 26207.

16. Bachhuka A, Christo SN, Cavallaro A, Diener KR, Mierczynska A, Smith LE, Marian R, Manavis J, Hayball JD, Vasilev K. Hybrid core/shell microparticles and their use for understanding biological processes. J. Colloid Interface Sci. 2015; 457: 9-17.

17. Visalakshan RM, Cavallaro AA, MacGregor MN, Lawrence EP, Koynov K, Hayball JD, Vasilev K. Nanotopography-Induced Unfolding of Fibrinogen Modulates Leukocyte Binding and Activation. Adv. Funct. Mater. 2019; 29 (14): 1807453.

18. Santos A, Aw MS, Bariana M, Kumeria T, Wang Y, Losic D. Drug-releasing implants: current progress, challenges and perspectives. Journal of Materials Chemistry B. 2014; 2 (37): 6157-6182.

19. Losic D, Simovic S. Self-ordered nanopore and nanotube platforms for drug delivery applications. Expert opinion on drug delivery. 2019; 2 (37): 6157-6182.

20. La Flamme KE, Popat KC, Leoni L, Markiewicz E, La Tempa TJ, Roman BB, Grimes CA, Desai TA. Biocompatibility of nanoporous alumina membranes for immunoisolation. Biomaterials 2007; 28 (16): 2638-2645.

21. Popat KC, Swan EEL, Mukhatyar V, Chatvanichkul KI, Mor GK, Grimes CA, Desai TA. Influence of nanoporous alumina membranes on long-term osteoblast response. Biomaterials 2005; 26 (22): 4516-4522.

22. Swan EEL, Popat KC, Desai TA. Peptide-immobilized nanoporous alumina membranes for enhanced osteoblast adhesion. Biomaterials. 2005; 26 (14): 1969-1976.

23. Popat KC, Chatvanichkul KI, Barnes GL, Latempa Jr TJ, Grimes CA, Desai TA. Osteogenic differentiation of marrow stromal cells cultured on nanoporous alumina surfaces. J. Biomed. Mater. Res. A. 2007; 80 (4): 955-964.

24. Karlsson M, Pålsgård E, Wilshaw PR, Di Silvio L. Initial in vitro interaction of osteoblasts with nano-porous alumina. Biomaterials. 2003; 24 (18): 3039-3046.

25. Michelmore A, Martinek P, Sah V, Short RD, Vasilev K. Surface Morphology in the Early Stages of Plasma Polymer Film Growth from Amine-Containing Monomers. Plasma Processes and Polymers. 2011; 8 (5): 367-372.

26. Hernandez-Lopez J, Bauer R, Chang WS, Glasser G, Grebel-Koehler D, Klapper M, Kreiter M, Leclaire J, Majoral JP, Mittler S. Functional polymers as nanoscopic building blocks. Materials Science and Engineering: C 2003; 23 (1-2): 267-274.

27. Rinsch CL, Chen XL, Panchalingam V, Eberhart RC, Wang JH, Timmons RB. Pulsed radio frequency plasma polymerization of allyl alcohol: Controlled deposition of surface hydroxyl groups. Langmuir. 1996; 12 (12): 2995-3002.

28. Michelmore A, Steele DA, Whittle JD, Bradley JW, Short RD. Nanoscale deposition of chemically functionalised films via plasma polymerisation. Rsc Advances. 2013; 3 (33): 13540-13557.

29. Coad BR, Scholz T, Vasilev K, Hayball JD, Short RD, Griesser HJ. Functionality of proteins bound to plasma polymer surfaces. ACS applied materials & interfaces. 2012; 4 (5): 2455-2463.

30. Goreham RV, Mierczynska A, Pierce M, Short RD, Taheri S, Bachhuka A, Cavallaro A, Smith LE, Vasilev K. A substrate independent approach for generation of surface gradients. Thin Solid Films. 2013; 528: 106-110.

31. Vasilev K, Poulter N, Martinek P, Griesser HJ. Controlled release of levofloxacin sandwiched between two plasma polymerized layers on a solid carrier. ACS Applied Materials & Interfaces 2011; 3 (12): 4831-4836.

32. Wahono SK, Cavallaro A, Vasilev K, Mierczynska A. Plasma polymer facilitated magnetic technology for removal of oils from contaminated waters. Environ. Pollut. 2018; 240: 725-732.

33. Mierczynska-Vasilev A, Boyer P, Vasilev K, Smith PA. A novel technology for the rapid, selective, magnetic removal of pathogenesis-related proteins from wines. Food Chem. 2017; 232: 508-514.

34. Cavallaro A, Vasilev K. Controlled and sustained release of pharmaceuticals via single step solvent-free encapsulation. Chem. Commun. 2015; 51 (10): 1838-1841.

35. Masuda H, Fukuda K. Ordered metal nanohole arrays made by a two-step replication of honeycomb structures of anodic alumina. Science. 1995; 268 (5216): 1466-1468.

36. Nielsch K, Choi J, Schwirn K, Wehrspohn RB, Gösele U. Self-ordering regimes of porous alumina: the 10 porosity rule. Nano Lett. 2002; 2 (7): 677-680.

37. Lee W, Park S-J. Porous anodic aluminum oxide: anodization and templated synthesis of functional nanostructures. Chem. Rev. 2014; 114 (15): 7487-7556.

38. Santos A, Kumeria T, Losic D. Nanoporous anodic aluminum oxide for chemical sensing and biosensors. TrAC, Trends Anal. Chem. 2013; 44: 25-38.

39. Chanput W, Mes J, Vreeburg RAM, Savelkoul HFJ, Wichers HJ. Transcription profiles of LPS-stimulated THP-1 monocytes and macrophages: a tool to study inflammation modulating effects of food-derived compounds. Food & Function. 2010; 1 (3): 254-261.

40. Chanput W, Mes JJ, Savelkoul HFJ, Wichers HJ. Characterization of polarized THP-1 macrophages and polarizing ability of LPS and food compounds. Food & Function. 2013; 4 (2): 266-276.

41. Chanput W, Mes JJ, Wichers HJ. THP-1 cell line: An in vitro cell model for immune modulation approach. International Immunopharmacology. 2014; 23 (1): 37-45.

42. Kessel A, Ben-Tal N. Introduction to proteins: structure, function, and motion. CRC Press. 2010.

43. Zheng K, Kapp M, Boccaccini AR. Protein interactions with bioactive glass surfaces: A review. Applied Materials Today. 2019; 15: 350-371.

44. Visalakshan RM, MacGregor MN, Cavallaro AA, Sasidharan S, Bachhuka A, Vasilev AM, Hayball JD, Vasilev K. Creating Nano-engineered Biomaterials with Well-Defined Surface Descriptors. ACS Applied Nano Materials. 2018; 1 (6): 2796-2807.

45. Mierczynska-Vasilev A, Mierczynski P, Maniukiewicz W, Visalakshan RM, Vasilev K, Smith PA. Magnetic separation technology: Functional group efficiency in the removal of haze-forming proteins from wines. Food Chemistry. 2019; 275: 154-160.

46. Bachhuka A, Hayball J, Smith LE, Vasilev K. Effect of surface chemical functionalities on collagen deposition by primary human dermal fibroblasts. ACS Applied Materials & Interfaces. 2015; 7 (42): 23767-23775.

47. Bachhuka A, Hayball JD, Smith LE, Vasilev K. The interplay between surface nanotopography and chemistry modulates collagen I and III deposition by human dermal fibroblasts. ACS Applied Materials & Interfaces. 2017; 9 (7): 5874-5884.

48. Kamath S, Bhattacharyya D, Padukudru C, Timmons RB, Tang L. Surface chemistry influences implant-mediated host tissue responses. J. Biomed. Mater. Res. A. 2008; 86 (3): 617-626.

49. Barbosa JN, Madureira P, Barbosa MA, Aguas AP. The influence of functional groups of self-assembled monolayers on fibrous capsule formation and cell recruitment. J. Biomed. Mater. Res. A. 2006; 76 (4): 737-743.

50. Damanik FFR, Rothuizen TC, van Blitterswijk C, Rotmans JI, Moroni L. Towards an in vitro model mimicking the foreign body response: tailoring the surface properties of biomaterials to modulate extra-cellular matrix. Sci. Rep. 2014; 4: 6325.

51. Ferraz N, Hong J, Santin M, Karlsson Ott M. Nanoporosity of alumina surfaces induces different patterns of activation in adhering monocytes/macrophages. International journal of biomaterials. 2010; 2010: 1-8.

52. Pujari S, Hoess A, Shen J, Thormann A, Heilmann A, Tang L, Karlsson-Ott M. Effects of nanoporous alumina on inflammatory cell response. J. Biomed. Mater. Res. A. 2014; 102 (11): 3773-3780.

53. Roach P, Eglin D, Rohde K, Perry CC. Modern biomaterials: a review—bulk properties and implications of surface modifications. J. Mater. Sci. Mater. Med. 2007; 18 (7): 1263-1277.

54. Wilson CJ, Clegg RE, Leavesley DI, Pearcy MJ. Mediation of biomaterial–cell interactions by adsorbed proteins: a review. Tissue Eng. 2005; 11 (1-2): 1-18.

55. Chen CZ, Raghunath M. Focus on collagen: in vitro systems to study fibrogenesis and antifibrosis _ state of the art. Fibrogenesis & Tissue Repair. 2009; 2 (1): 7.

56. Holt DJ, Grainger DW. Multinucleated giant cells from fibroblast cultures. Biomaterials. 2011; 32 (16): 3977-3987.

57. Kamath S, Bhattacharyya D, Padukudru C, Timmons RB, Tang L. Surface chemistry influences implant-mediated host tissue responses. J. Biomed. Mater. Res. A. 2008; 86A (3): 617-626.

58. Eaton JW, Tang L. Inflammatory Responses to Biomaterials. Am. J. Clin. Pathol. 1995; 103 (4): 466-471.

59. Moreira M, Fagundes DJ, Simões MdJ, Taha MO, Perez LMN, Bazotte RB. The effect of liposome-delivered prednisolone on collagen density, myofibroblasts, and fibrous capsule thickness around silicone breast implants in rats. Wound Repair Regen. 2010; 18 (4): 417-425.

60. Avula M, Jones D, Rao AN, McClain D, McGill LD, Grainger DW, Solzbacher F. Local release of masitinib alters in vivo implantable continuous glucose sensor performance. Biosens. Bioelectron. 2016; 77: 149-156.

61. Kastellorizios M, Papadimitrakopoulos F, Burgess DJ. Multiple tissue response modifiers to promote angiogenesis and prevent the foreign body reaction around subcutaneous implants. J. Control. Release. 2015; 214: 103-111.

62. Shin YN, Kim BS, Ahn HH, Lee JH, Kim KS, Lee JY, Kim MS, Khang G, Lee HB. Adhesion comparison of human bone marrow stem cells on a gradient wettable surface prepared by corona treatment. Appl. Surf. Sci. 2008; 255 (2): 293-296.

63. Tang L, Thevenot P, Hu W. Surface chemistry influences implant biocompatibility. Curr. Top. Med. Chem. 2008; 8 (4): 270-280.

64. Liu X, Feng Q, Bachhuka A, Vasilev K. Surface modification by allylamine plasma polymerization promotes osteogenic differentiation of human adipose-derived stem cells. ACS Applied Materials & Interfaces. 2014; 6 (12): 9733-9741.

65. Liu X, Feng Q, Bachhuka A, Vasilev K. Surface chemical functionalities affect the behavior of human adipose-derived stem cells in vitro. Appl. Surf. Sci. 2013; 270: 473-479.

66. Hulander M, Lundgren A, Berglin M, Ohrlander M, Lausmaa J, Elwing H. Immune complement activation is attenuated by surface nanotopography. International Journal of Nanomedicine. 2011; 6: 2653-2666.

67. Bachhuka A, Delalat B, Ghaemi SR, Gronthos S, Voelcker NH, Vasilev K. Nanotopography mediated osteogenic differentiation of human dental pulp derived stem cells. Nanoscale. 2017; 9 (37): 14248-14258.

68. Liu X, Xie Y, Shi S, Feng Q, Bachhuka A, Guo X, She Z, Tan R, Cai Q, Vasilev K. The co-effect of surface topography gradient fabricated via immobilization of gold nanoparticles and surface chemistry via deposition of plasma polymerized film of allylamine/acrylic acid on osteoblast-like cell behavior. Appl. Surf. Sci. 2019; 473: 838-847.

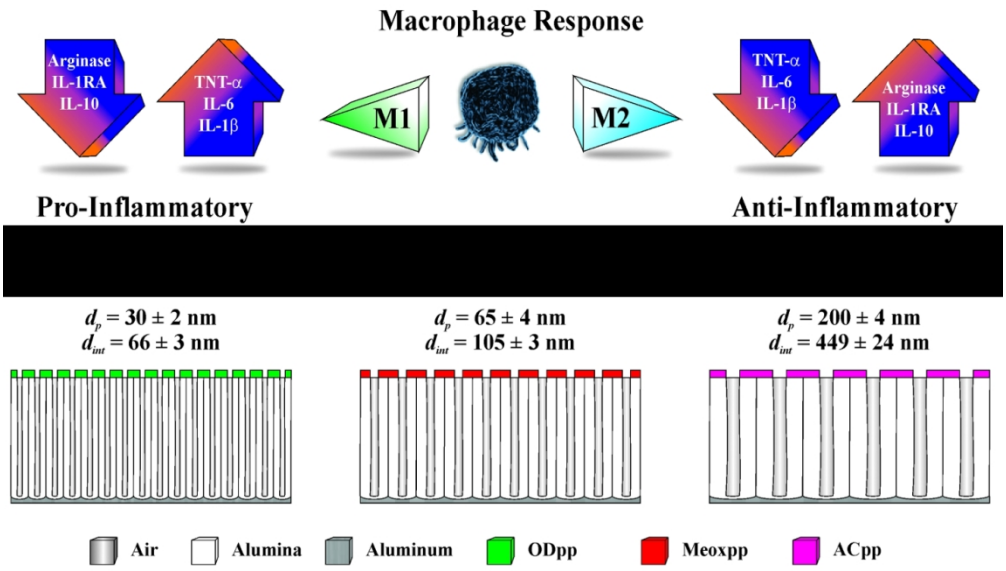


Schematic representation of macrophage polarization (M1 and M2 phenotypes) on chemically and nanotopographically modified surfaces.

247x145mm (150 x 150 DPI)